

ENERGY ESTIMATES FOR DISCRETIZATION ERRORS IN WATER HAMMER PROBLEMS

By Mohamed S. Ghidaoui,¹ Bryan W. Karney,² Member, ASCE, and Duncan A. McInnis³

ABSTRACT: An integrated energy approach is developed for transient problems in pipelines using the fixed-grid method of characteristics. The goal is to understand how discretization errors associated with common interpolation schemes arise and how these errors can be controlled. Specifically, new analytical energy expressions demonstrate that both time-line and space-line interpolation attenuate the total energy of the system; in contrast, the wave-speed adjustment approach preserves the total energy but distorts the partitioning between kinetic and internal energy. The analytic results are confirmed through numerical studies of several series pipe systems. Both the numerical experiments and the mathematical expressions show that the discretization errors are small and can be ignored as long as the work in the system is continuous and substantial. When the work is small or negligible, however, a Courant number C_r value close to 1 is required to control the numerical dissipation.

INTRODUCTION

The most popular method for analyzing transient conditions in multipipe systems is the fixed-grid method of characteristics (FGMOC). To apply boundary conditions at the junction of two or more pipes, the time step Δt must be common to all pipes. The common time step, however, makes it difficult to achieve an integer number of reaches in each pipe. To understand this, consider that the time step determines the distance traveled by a wave in pipe p as $\Delta x_p = c_p \Delta t$ for $p = 1, \dots, n$ where c_p is the wave speed and n is the number of pipes in the system. Therefore, the number of reaches in pipe p is $N_p = L_p / \Delta x_p = L_p / c_p \Delta t$. Since pipes generally have a variety of wave speeds and lengths, it is unlikely that N_p will be a natural number for all pipes. To deal with this discretization problem, one can either adjust the wave speed, thus forcing an integer number of reaches, or interpolate between grid points, thereby allowing N_p to be a non-integer (Karney and Ghidaoui 1997).

Over the last 20 years, several researchers have studied the dispersion and dissipation characteristics of various discretization approaches to the FGMOC using Fourier methods (Wiggert and Sundquist 1977; Goldberg and Wylie 1983). Unfortunately, Fourier methods lack essential boundary condition information, ignore the influence of the wave profile on the numerical errors, assume that the initial conditions are periodic, and are restricted to linear numerical models with constant coefficients (O'Brian et al. 1951; Damuller et al. 1989; Samuels and Skeels 1990; Sibetheros et al. 1991). Therefore, Fourier methods cannot be used as the only benchmark for selecting the most appropriate numerical scheme for nonlinear boundary-value hyperbolic problems. When the exact solution is known, L_1 and L_2 norms have been used to evaluate the numerical errors associated with the solution of the water hammer equations by the MacCormack, Lambda, and Gabutti schemes (Chaudhry and Hussaini 1985). However, the L_1 and L_2 norms do not measure a physical property such as mass or energy, thereby complicating the interpretation and comparison of results. Based on a single pipe with fixed Courant num-

ber subject to sudden closure downstream, Sibetheros et al. (1991) used three dimensionless parameters to study the discretization errors; however, the specific nature of the numerical tests makes it difficult to generalize their method to more complex applications (Karney and Ghidaoui 1992). More recently, Ghidaoui and Karney (1994) developed the concept of equivalent partial differential equations for the water hammer equations.

In this paper, the integrated form of the mechanical energy equation is used to provide a quantitative assessment of various discretization options, including time and space-line interpolation and wave speed adjustment, for a set of series-connected pipes. Energy plots are used to provide insight into the dissipative nature of time and space-line interpolation schemes. The ratio of the total energy at time t to the total energy at time zero becomes a natural measure of the numerical dissipation, particularly when the physical energy dissipation and the work at the boundary are small. Further, the energy portraits illustrate the smoothing of sharp waves by interpolation. This numerical dissipation does not always arise in the wave speed adjustment approach, as is shown theoretically and illustrated by examples. The energy approach has the advantage of allowing the transient analyst to determine the numerical dissipation in complex and realistic pipeline systems.

CHARACTERISTIC EQUATIONS

The pressure fluctuations created by a flow disturbance in a closed conduit propagate as pulse waves throughout the pipe length. If the friction force is modeled by the steady state Darcy-Weisbach equation, and the pipe has a circular cross section, the derivation of the momentum and continuity equations is given in standard references (e.g., Wylie and Streeter 1993; Chaudhry 1987). Coupling these equations along the characteristic lines (e.g., Ghidaoui and Karney 1995) produces the following characteristic form:

$$\frac{dH}{dt} \pm B \frac{dQ}{dt} + \frac{Bf^\pm}{2D_a A} Q|Q| = 0 \quad \text{along} \quad \frac{dx}{dt} = \pm c \quad (1)$$

in which t = time; x = distance along pipe centerline; $H = H(x, t)$ = piezometric head (i.e., sum of the pressure head and elevation head); $Q = Q(x, t)$ = volumetric rate of flow or discharge; A = cross-sectional area of a pipe with diameter D_a ; c = wave speed; $B = c/gA$, where g = acceleration due to gravity; and f^\pm = friction factor along positive and negative characteristic lines, respectively. When the Reynolds number is very high, the friction factors f^+ and f^- can usually be assigned a single constant value of f . The derivation of these equations assumes that the fluid is slightly compressible, the pipe is elas-

¹Asst. Prof., Dept. of Civ. and Struct. Engrg., Hong Kong Univ. of Sci. and Technol., Hong Kong, China.

²Prof., Dept. of Civ. Engrg., Univ. of Toronto, 5 King's College Rd., Toronto, Canada M5S 1A4.

³Tech. Program Mgr., Res. Ctr., Hong Kong Univ. of Sci. and Technol., Hong Kong, China.

Note. Discussion open until September 1, 1998. To extend the closing date one month, a written request must be filed with the ASCE Manager of Journals. The manuscript for this paper was submitted for review and possible publication on July 28, 1996. This paper is part of the *Journal of Hydraulic Engineering*, Vol. 124, No. 4, April, 1998. ©ASCE, ISSN 0733-9429/98/0004-0384-0393/\$4.00 + \$.50 per page. Paper No. 11271.

tic, the convective terms are negligible, and the flow is one-dimensional.

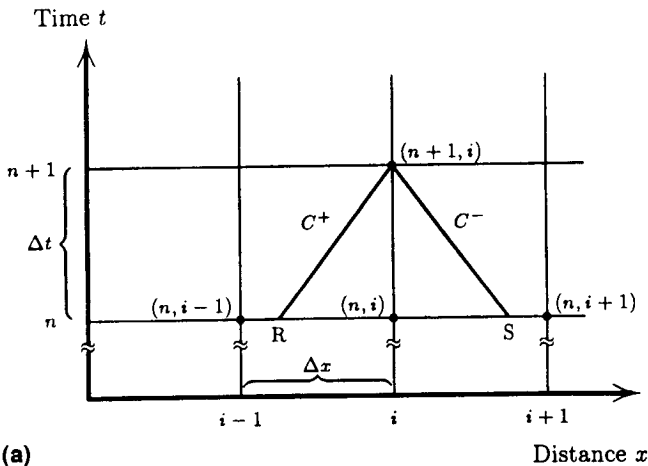
For a single pipe, the FGMOC solution of (1) on the grids shown in Fig. 1 is

$$H_i^{n+1} = \frac{1}{2}(H_R + H_S) + \frac{B}{2}(Q_R - Q_S) - \frac{Bf}{2D_a A} \left(\int_R^{n+1} Q|Q| dt + \int_S^{n+1} Q|Q| dt \right) \quad (2)$$

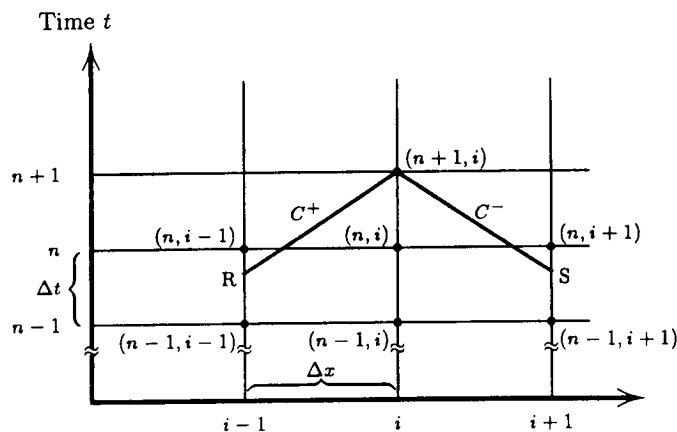
$$BQ_i^{n+1} = \frac{1}{2}(H_R - H_S) + \frac{B}{2}(Q_R + Q_S) - \frac{Bf}{2D_a A} \left(\int_R^{n+1} Q|Q| dt - \int_S^{n+1} Q|Q| dt \right) \quad (3)$$

in which the subscript i and superscript $n + 1$ indicate the spatial and temporal locations, respectively, of the grid point with coordinates $[i\Delta x, (n + 1)\Delta t]$. The subscripts R and S are intermediate positions at the foot of the positive and negative characteristic lines; that is R and S are found by interpolating known values from earlier time steps. Eqs. (2) and (3) relate exclusively to internal sections and are therefore valid only for $i = 1, \dots, m - 1$, where m is the total number of pipe reaches. Extensions of these equations to a series pipe system are conceptually straightforward, though notationally more demanding; in essence, the procedure is to index constraints to particular pipes and then to sum the energy terms over each pipe in the system.

To obtain conditions at the upstream and downstream



(a)



(b)

FIG. 1. FGMOC Grid for: (a) Space-Line Interpolation; (b) Time-Line Interpolation

boundaries, equations describing the head and flow at these ends must be coupled with the following characteristic forms:

$$H_0^{n+1} - BQ_0^{n+1} = H_{S_1} - BQ_{S_1} - \frac{Bf}{2D_a A} \int_{S_1}^{n+1} Q|Q| dt \quad (4)$$

$$H_m^{n+1} + BQ_m^{n+1} = H_{R_m} + BQ_{R_m} - \frac{Bf}{2D_a A} \int_{R_m}^{n+1} Q|Q| dt \quad (5)$$

where S_1 and R_m are interpolated values in the first and last section, respectively, of each pipe. Solutions for many boundary conditions, as well as an explicit set of approximations for the integration of the friction term, are found in Karney and McInnis's (1992) study and in standard references.

Transient Energy Equation

In this section, the mechanical energy expressions associated with the FGMOC in a series-connected pipe system are presented. For convenience, the concept of an inner product of two functions is introduced. To do this, let ψ and ζ be two arbitrary functions that are either continuous or piecewise continuous on the interval $[0, L]$. The inner product of ψ with ζ is $\langle \psi, \zeta \rangle = \int_0^L \psi \zeta dx$. If ψ and ζ are discrete functions given at nodes $i = 0, \dots, m$, where m is the number of intervals (i.e., reaches in a pipe segment), then the second-order discrete inner product of ψ with ζ is

$$\langle \psi, \zeta \rangle = \Delta x \left[\frac{\psi_0 \zeta_0 + \psi_m \zeta_m}{2} + \sum_{i=1}^{m-1} \psi_i \zeta_i \right]$$

where Δx = reach length and ψ_i and ζ_i are the values of ψ and ζ at node i . The square root of the inner product of a function ψ with itself is called the norm of ψ and is represented by $\|\psi\|$.

Taking the momentum and continuity equations as a basis, Karney (1990) developed the following integrated expression for the total energy in the system:

$$\frac{dU}{dt} + \frac{dT}{dt} + W' + D' = 0 \quad (6)$$

in which $U = \rho(H, H)/2AB^2$ = total internal energy; $T = \rho(Q, Q)/2A$ = total kinetic energy; $W' = \rho g Q(L, t)H(L, t) - \rho g Q(0, t)H(0, t)$ = net rate at which work is being done on fluid; and $D' = \rho f \langle |Q|, Q^2 \rangle / 2D_a A^2$ = rate of viscous dissipation. The term "internal energy" is used to describe the energy associated with fluid density and pipeline elasticity effects.

To determine the internal energy at time $n + 1$, the discrete inner product of the head function H_i^{n+1} with itself is calculated, where H_i^{n+1} for $i = 1, \dots, m - 1$ is given by (2), and the terminal heads H_0^{n+1} and H_m^{n+1} are found by solving (4) and (5), respectively. As is typical for studies of errors, the friction factor f is set to zero for these manipulations. Performing the inner product and utilizing (2) results in the following expression:

$$\begin{aligned} \|H^{n+1}\|^2 &= \frac{1}{4} (\|H_R\|^2 + \|H_S\|^2 + B^2\|Q_R\|^2 + B^2\|Q_S\|^2) \\ &+ \frac{1}{2} (\langle H_R, H_S \rangle - B^2\langle Q_R, Q_S \rangle) + \frac{B}{2} (\langle Q_R, H_R + H_S \rangle \\ &- \langle Q_S, H_R + H_S \rangle) + \frac{\Delta x}{2} [(H_0^{n+1})^2 + (H_m^{n+1})^2] \end{aligned} \quad (7)$$

in which the norms and inner products for the interpolated variables are appropriately adjusted. Similarly, the kinetic energy at time $n + 1$ is obtained from the inner product of the flow function Q^{n+1} [i.e., (3) with $f = 0$] with itself. Rearranging and simplifying results in the following expression:

$$\begin{aligned}
B^2 \|Q^{n+1}\|^2 &= \frac{1}{4} (\|H_R\|^2 + \|H_S\|^2 + B^2 \|Q_R\|^2 + B^2 \|Q_S\|^2) \\
&+ \frac{1}{2} (-\langle H_R, H_S \rangle + B^2 \langle Q_R, Q_S \rangle) + \frac{B}{2} (\langle H_R, Q_R + Q_S \rangle \\
&- \langle H_S, Q_R + Q_S \rangle) + \frac{B^2}{2} [(Q_0^{n+1})^2 + (Q_m^{n+1})^2] \Delta x
\end{aligned} \quad (8)$$

The total mechanical energy E^{n+1} at time level $n + 1$ is obtained by summing the expressions for internal and kinetic terms (with suitable unit conversions and cancellations) to obtain

$$\begin{aligned}
E^{n+1} &= \frac{\rho}{4A} \left\{ \left(\frac{1}{B} \right)^2 (\|H_R\|^2 + \|H_S\|^2) + \|Q_R\|^2 + \|Q_S\|^2 \right. \\
&+ \frac{2}{B} (\langle H_R, Q_R \rangle - \langle H_S, Q_S \rangle) + \left(\frac{1}{B} \right)^2 [(H_0^{n+1})^2 + (H_m^{n+1})^2] \Delta x \\
&\left. + (Q_0^{n+1})^2 \Delta x + (Q_m^{n+1})^2 \Delta x \right\}
\end{aligned} \quad (9)$$

To solve (2) and (3), the head and flow at R and S must be known. Ideally, R and S should coincide with nodes for which the head and flow have already been computed. However, as has been argued, the application of the FGMOC to a set of pipes with different lengths and wave speeds generally eliminates this possibility, thus creating a discretization problem. This problem was discussed in some detail, along with a number of novel attempts at resolving it, by Karney and Ghidaoui (1997). In what follows, the errors associated with the wave-speed adjustment approach, as well as with the conventional space-line and time-line interpolation strategies, are investigated through the energy equation.

Energy Equation for Wavespeed Adjustment

The wave speed variation methodology is often justified by the uncertainty in the wave speed values (Wylie and Streeter 1993; Chaudhry 1987). Therefore, the wave speed is simply an estimated value within a range of possible speeds. Moreover, numerical experiments have confirmed that peak pressure magnitudes are relatively insensitive to assumed values of wave speed, particularly in systems in which the changes in boundary conditions are slow relative to the wave travel time. Although it was reported that the maximum permissible variation of the wave speed should be limited to 15% (Wylie and Streeter 1993), there is little theoretical basis for this rule.

The ϕ -index (or "compressibility index") approach (Karney 1990) is another way of justifying the wave-speed adjustment approach. The ϕ -index is defined as the ratio of the change in internal energy to the change in kinetic energy. Karney (1990) argues that as the compressibility index becomes smaller, the transient behavior of the system becomes independent of the wave speed, thus justifying a variation in wave speed. In most water hammer problems, however, the ϕ -index is not small, therefore, wave speed adjustment is seldom justified solely on this basis.

The present paper shows that in a particular sense the wave speed adjustment method conserves energy. More specifically, the sum of the kinetic and internal energies plus the work and dissipation is independent of wave speed. Moreover, the equations of motion in an adjusted wave speed system are still represented by a continuous mathematical model, avoiding any dissipation that may have otherwise existed. The mathematical proof is now presented.

If the datum is set so that there is initially little or no internal energy in the system, then (6) can be integrated for a known

wave speed c in the interval of time $[0, t]$. The result is the total energy for the system

$$U(t) + T(t) + \int_0^t (D' + W') d\tau + T(0) \quad (10)$$

If, instead of using the actual wave speed c , one uses the adjusted value \bar{c} , a similar equation may be derived

$$\bar{U}(t) + \bar{T}(t) + \int_0^t (\bar{D}' + \bar{W}') d\tau + \bar{T}(0) \quad (11)$$

But because the initial steady state energy of the system is independent of the value of the wave speed, $T(0) = \bar{T}(0)$. Therefore, (10) and (11) must be equal, justifying a limited claim of energy conservation. Of course, the equality of (10) and (11) is of only conceptual interest since it is usually impossible to represent the energy expressions analytically as a function of time. However, the result is interesting in that the selection of the wave speed obviously influences the shape and form of the piezometric head and flow profiles, and therefore the partitioning of energy between its various forms. Yet, even with this redistribution, the total overall energy conversion rate in the system is invariant and independent of wave speed.

Energy Equation for Space-Line Interpolation

Space-line interpolation approximates the solution to the FGMOC by linearly interpolating the dependent variables of Q and H at the time level $n\Delta t$ between spatial grid points $(i - 1)\Delta x$ and $i\Delta x$ for R and $i\Delta x$ and $(i + 1)\Delta x$ for S . That is,

$$\begin{aligned}
H_{R_i} &= C_r H_{i-1}^n + (1 - C_r) H_i^n, \quad Q_{R_i} = C_r Q_{i-1}^n + (1 - C_r) Q_i^n, \\
i &= 1, \dots, m
\end{aligned} \quad (12)$$

$$\begin{aligned}
H_{S_i} &= C_r H_{i+1}^n + (1 - C_r) H_i^n, \quad Q_{S_i} = C_r Q_{i+1}^n + (1 - C_r) Q_i^n, \\
i &= 0, \dots, m - 1
\end{aligned} \quad (13)$$

in which C_r is the grid Courant number, and the subscript i and the superscript n indicate the spatial and temporal locations, respectively, of the current grid point. Because the required expressions are numerous, expansions of the various inner product terms in (9) are given in Appendix I. Inserting these expressions into (9) and simplifying yields

$$\begin{aligned}
E^{n+1} &= (1 + 2C_r^2 - 2C_r) E^n \\
&+ C_r (1 - C_r) \frac{\rho}{2A} \left[\left(\frac{1}{B} \right)^2 \langle H_i^n, H_{i+1}^n \rangle + \langle Q_i^n, Q_{i+1}^n \rangle \right] - W
\end{aligned} \quad (14)$$

where

$$E^n = \frac{\rho}{2A} \left[\left(\frac{1}{B} \right)^2 \|H^n\|^2 + \|Q^n\|^2 \right] \quad (15)$$

and

$$W = \rho g \Delta t (Q_m^{n+1} H_m^{n+1} - Q_0^{n+1} H_0^{n+1} + Q_{R_i} H_{R_i} - Q_{S_{m-1}} H_{S_{m-1}}) \quad (16)$$

The Cauchy-Schwartz inequality implies that $\langle H_i^n, H_{i+1}^n \rangle \leq \|H_i^n\|^2$ and $\langle Q_i^n, Q_{i+1}^n \rangle \leq \|Q_i^n\|^2$. Therefore, a new parameter can be defined as

$$\beta^n = \frac{\rho}{2A} \left[\left(\frac{1}{B} \right)^2 \langle H_i^n, H_{i+1}^n \rangle + \langle Q_i^n, Q_{i+1}^n \rangle \right] \frac{1}{E^n} \leq 1 \quad (17)$$

which is a function of the wave profile. For example, for a constant head profile β is clearly equal to 1. Moreover, at the sudden stoppage of flow, the velocity goes from a steady value

to zero across the jump. Therefore, with a suitable choice of datum, either H_{i+1}^n or H_i^n is zero and either Q_{i+1}^n or Q_i^n is zero. The net result is that $\beta = 0$ for such a step wave.

If the work $W = 0$ in (14), the following form results:

$$\frac{E^{n+1}}{E^n} = 1 + C_r(\beta^n - 1)(1 - C_r) \leq 1 \quad (18)$$

Eq. (18) shows that space-line interpolation dissipates energy and that this dissipation is a function of both C_r and the wave profile. In addition, as the wave profile becomes progressively smoother, β approaches unity and the resulting numerical dissipation reduces. Furthermore, as C_r approaches unity, the dissipation factor $1 + C_r(\beta^n - 1)(1 - C_r)$ tends to 1. By contrast, if C_r exceeds 1, the right-hand side of (18) also exceeds 1, implying that the energy increases with time. Yet, without work, there should be no energy input in (18) and the growth of energy must be due to numerical instability, thus providing an independent check of the Courant condition.

Energy Equation for Time-Line Interpolation

Time-line interpolation approximates the solution to the FGMOC by linearly interpolating the dependent variables of Q and H between grid points $[(i - 1)\Delta x, n\Delta t]$ and $[(i - 1)\Delta x, (n - 1)\Delta t]$ for R and $[(i + 1)\Delta x, n\Delta t]$ and $[(i + 1)\Delta x, (n - 1)\Delta t]$ for S . The result is

$$H_{R_i} = (1 - \xi)H_{i-1}^n + \xi H_{i-1}^{n-1}, \quad Q_{R_i} = (1 - \xi)Q_{i-1}^n + \xi Q_{i-1}^{n-1}, \quad (19)$$

$$i = 1, \dots, m$$

$$H_{S_i} = (1 - \xi)H_{i+1}^n + \xi H_{i+1}^{n-1}, \quad Q_{S_i} = (1 - \xi)Q_{i+1}^n + \xi Q_{i+1}^{n-1}, \quad (20)$$

$$i = 0, \dots, m - 1$$

in which ξ is equal to $(1 - C_r)/C_r$, and the subscript i and the superscript n indicate the spatial and temporal location of the current grid point, respectively. Inserting these expressions into (9) and simplifying yields

$$E^{n+1} = \frac{(2C_r - 1)^2}{C_r^2} E^n + \xi^2 E^{n-1} + \frac{2\rho\xi(2C_r - 1)}{AC_r} \left[\left(\frac{1}{B}\right)^2 \langle H_i^n, H_i^{n-1} \rangle + \langle Q_i^n, Q_i^{n-1} \rangle \right] - W \quad (21)$$

where E^n is given by (15); E^{n-1} is also the mechanical energy, but at the previous time step; and W is still given by (16), although the interpolated values are now based on the time-line equations.

Through use of the Cauchy-Schwartz inequality, an estimate for the energy E^{n+1} can be derived. The result is

$$E^{n+1} \leq \frac{(2C_r - 1)^2}{C_r^2} E^n + \frac{(1 - C_r)^2}{C_r^2} E^{n-1} + \frac{2(1 - C_r)(2C_r - 1)}{C_r^2} \max(E^{n-1}, E^n) - W \quad (22)$$

Letting $F^{n+1} = E^n$ allows (22) to be written in a matrix form, which is more convenient for stability analysis. If $\max(E^{n-1}, E^n) = E^{n-1}$, then

$$\begin{pmatrix} E^{n+1} \\ F^{n+1} \end{pmatrix} \leq \begin{pmatrix} \frac{(2C_r - 1)^2}{C_r^2} & \frac{(1 - C_r)^2 + 2(1 - C_r)(2C_r - 1)}{C_r^2} \\ 1 & 0 \end{pmatrix} \begin{pmatrix} E^n \\ F^n \end{pmatrix} - \begin{pmatrix} W \\ 0 \end{pmatrix} \quad (23)$$

If $\max(E^{n-1}, E^n) = E^n$, then

$$\begin{pmatrix} E^{n+1} \\ F^{n+1} \end{pmatrix} \leq \begin{pmatrix} \frac{(2C_r - 1)^2 + 2(1 - C_r)(2C_r - 1)}{C_r^2} & \frac{(1 - C_r)^2}{C_r^2} \\ 1 & 0 \end{pmatrix} \begin{pmatrix} E^n \\ F^n \end{pmatrix} - \begin{pmatrix} W \\ 0 \end{pmatrix} \quad (24)$$

The stability of time-line interpolation can be deduced from the form of (23) and (24). Stability is guaranteed if each eigenvalue of the two matrices is less than or equal to 1. This is always the case as long as $C_r \leq 1$. Yet, $C_r < 1$ implies that the diagonal matrices (with eigenvalues as the diagonal entries) are contraction matrices; therefore, time-line interpolation is a dissipative scheme. Furthermore, the energy estimate method clearly shows how the interpolation affects the work term at the boundary, thus overcoming a weakness of the Fourier approach.

Eqs. (23) and (24) also indicate that both numerical errors are a function of the Courant number and the wave profile. For instance, the discretization error is eliminated when C_r is either 1 or 1/2. In addition, the numerical dissipation is minimized when the head and flow functions are smooth and relatively linear. In fact, the third term on the right-hand side of (21) clearly shows the dependence on wave profile.

Analysis for Sudden Closure

If the downstream valve in a series pipe system closes suddenly and completely, no work will be done at the valve. In addition, if the steady state is duplicated in order to initiate analysis, $E^{-1} = E^0$. Several cases related to the dissipation can now be identified.

1. If $0.95 \leq C_r \leq 1$ then $(2C_r - 1)^2/C_r^2 \geq 0.9$. This implies that the second and third terms on the right-hand side of (22) make up less than 10% of the right-hand side, allowing the following approximation to be made for the full energy cascade:

$$E^n \approx \left[\frac{(2C_r - 1)^2}{C_r^2} \right]^n E^0 \quad (25)$$

2. If $0.5 \leq C_r \leq 0.6$, then $(2C_r - 1)^2/C_r^2 \geq 0.11$. This implies that the second and third terms on the right-hand side of (22) make up more than 90% of the right-hand side. Thus, the following approximation can be made:

$$E^n \approx \left[1 - \frac{(2C_r - 1)^2}{C_r^2} \right]^n E^0 \quad (26)$$

Eqs. (25) and (26) are approximate theoretical relations for calculating the numerical energy dissipation in problems such as sudden valve closure. Moreover, problems with no work tend to produce the largest rates of numerical energy dissipation since no physical wave smoothing occurs. For this reason, (25) and (26) provide a simple and practical upper-bound estimate for the numerical dissipation even in more complicated problems.

3. Finally, if $0.6 \leq C_r \leq 0.95$, then a more complicated expression is required:

$$E^n \approx \left[1 + (\gamma^n - 1) \frac{2(1 - C_r)(2C_r - 1)}{C_r^2} \right]^n E^0 \quad (27)$$

where

$$\gamma^n = \frac{\frac{\rho}{2A} \left[\left(\frac{1}{B}\right)^2 \langle H_i^n, H_i^{n-1} \rangle + \langle Q_i^n, Q_i^{n-1} \rangle \right]}{E^{n-1}} \quad (28)$$

When steady state conditions prevail or when the transient is slow, the heads and flows at one time level will

be nearly equal to those at the next time level. Thus, γ^n will be close to 1 and the energy dissipation predicted by (27) will be minimal. For more abrupt transitions, however, substantial rates of energy dissipation may occur.

The case of sudden closure also makes it possible to more directly compare space-line and time-line interpolation. For this example, both β^n and γ^n coefficients are expected to have the same magnitude. Using (18) and (27) one can estimate the conditions under which space-line interpolation is expected to perform better than time-line interpolation and vice-versa. In general, space-line interpolation will have less dissipation only if

$$\frac{C_r(1 - C_r)}{[2(1 - C_r)(2C_r - 1)]/C_r^2} \leq 1 \quad (29)$$

a condition that is true if $0.54 \leq C_r \leq 1$. However, intensive numerical experimentation does indicate that this requirement is a necessary, but not sufficient, condition. In fact, numerical results suggest that space-line interpolation outperforms time-line interpolation for $C_r > 0.6$.

Further insight can be obtained by comparing β^n to γ^n for time-line and space-line interpolation. The ratio of these two quantities is as follows:

$$\frac{\gamma^n}{\beta^n} = \frac{\frac{\rho}{2A} \left[\left(\frac{1}{B} \right)^2 \langle H_i^n, H_i^{n-1} \rangle + \langle Q_i^n, Q_i^{n-1} \rangle \right]}{E^{n-1}} \quad (30)$$

$$\frac{\frac{\rho}{2A} \left[\left(\frac{1}{B} \right)^2 \langle H_i^n, H_{i+1}^n \rangle + \langle Q_i^n, Q_{i+1}^n \rangle \right]}{E^n}$$

Space-line interpolation is a better approximation than time-line interpolation if ratio (30) is larger than 1. This is usually the case for two reasons. First, with W and D equal to zero, $E^n \leq E^{n-1}$ due to numerical dissipation. More importantly, $\langle H_i^n, H_i^{n-1} \rangle/B^2 + \langle Q_i^n, Q_i^{n-1} \rangle$ is less than or equal to $\langle H_i^n, H_{i+1}^n \rangle/B^2 + \langle Q_i^n, Q_{i+1}^n \rangle$. These quantities are equal to each other for $t < L/c$. When $t \geq L/c$, the wave interacts with the boundary and reflects, causing a sign change in either head or flow. This means that the inner product $\langle H_i^n, H_i^{n-1} \rangle/B^2 + \langle Q_i^n, Q_i^{n-1} \rangle$ has a few negative values near the boundaries, making the overall magnitude of this quantity smaller than it should be. The sign reversal at the boundaries does not affect the inner product $\langle H_i^n, H_{i+1}^n \rangle/B^2 + \langle Q_i^n, Q_{i+1}^n \rangle$ since space-line interpolation does not use old boundary condition information.

It is difficult to draw general theoretical conclusions for valve motions more complicated than sudden closure. For this reason, a numerical case study is considered next.

NUMERICAL EXAMPLES

The case study consists of two pipes in series connected to an upstream reservoir and a downstream valve. The length of the upstream pipe is 800 m while the downstream pipe is 300 m long. For both pipes, the cross-sectional area is 1 m², the unadjusted wave speed is 1,000 m/s, friction factor $f = 0.0$ for the first two cases and 0.02 for the third case, and the steady state discharge is 1 m³/s. The datum for the hydraulic grade line is set at the surface of the reservoir so that an instantaneous valve closure produces no work.

The discretization strategy is based on the pipe that has the minimum wave travel time L/c (Karney and Ghidaoui 1997). Through selection of an integer number of reaches in this "shortest" pipe, N_{SP} , the time step becomes $\Delta t = (L/cN)_{SP}$, which equals $0.3/N_{SP}$ seconds in the current example. The approach of using at least one reach in the shortest pipe guarantees that the number of reachbacks in time-line interpolation

TABLE 1. Time Discretization in Example Two-Pipe System

N_{SP} (1)	Δt (2)	$L/c\Delta t$ (3)	\bar{c} (4)	C_r (5)	ξ (6)
1	0.300	2.667	888.8	0.7500	0.6667
2	0.150	5.334	1066.7	0.9375	0.9330
3	0.100	8.000	1000.0	1.0000	1.0000
5	0.060	13.334	1025.6	0.9750	0.9750

will not exceed one and that the Courant number is bounded by 0.5 and 1. The time step determines not only the Courant number, but also the required wave speed adjustment and the degree of interpolation in the other pipes. For the example system, these parameters are summarized in Table 1 for four values of N_{SP} (i.e., 1, 2, 3, and 5). Note that for the special case of $N_{SP} = 3$, both pipes are divided into an integer number of reaches and there are no discretization errors. This case is treated as a nominally "exact" case in the comparisons that follow. For the other values of N_{SP} in Table 1, a discretization error remains.

One advantage of the wave-speed adjustment method is also illustrated by this example. Since wave speeds can be chosen either slightly faster or slower than the true speed, the number of reaches in a pipe can be rounded to the nearest integer. By contrast, interpolation procedures must use the floor of $L/(c \cdot \Delta t)$ in order to satisfy the Courant condition. Due to the benefits of rounding, the proportional change in wave speed is often less than the required degree of interpolation. For example, with $N_{SP} = 1$, the change in wave speed (Table 1) is only 11%, whereas the required interpolation is 25% and 33% for space-line and time-line interpolation, respectively.

Case 1: Sudden Complete Valve Closure

If friction is set to zero, then the physical dissipation of internal energy is eliminated. Moreover, if the downstream valve is closed instantly, no fluid is exchanged with the environment across a pressure difference; therefore, this work is also equal to zero.

In the plots for this and the following examples, energy information is displayed as the total energy $E = U + T$ versus time t . In the test system, for example, the initial total energy is 550 kJ; if energy is conserved, a straight line parallel to the time axis will be plotted at the 550 kJ level. Any departure from a zero slope line represents either some kind of dissipation or work at the boundaries. In particular, if both physical work and dissipation are zero, then any dissipation arises solely due to the numerical interpolation. If both work and friction dissipation are nonzero, numerical dissipation can be obtained by comparing the energy curve corresponding to the "no interpolation" ($N_{SP} = 3$) solution with that of the approximate solution. Thus, the exact energy diagram for this case is a straight line parallel to the time axis and given by $E = 550$ kJ, as shown in Fig. 2. As was predicted theoretically, the energy diagram for the wave-speed adjustment approach is identical to the exact energy diagram when $W = 0$ and $D = 0$, regardless of the degree of adjustment. This is because wave-speed adjusted work and dissipation remain equal to zero.

In time-line interpolation the total energy E is conserved for the first $L/c = 300/1,000 = 0.3$ s and then decays rapidly towards the time axis (Fig. 2). Initially, energy is conserved because the wave is still in the downstream pipe in which $C_r = 1$. However, energy dissipation begins once the wave enters the upstream pipe in which $C_r < 1$. It is emphasized that this dramatic energy dissipation is purely numerical. For example, when $C_r = 0.94$, Fig. 2 shows that after 25 s of simulation almost 50% of the energy has been lost. The theoretical energy dissipation for $C_r = 0.94$ at $t = 25$ s (i.e., after $n = 25/0.15 =$

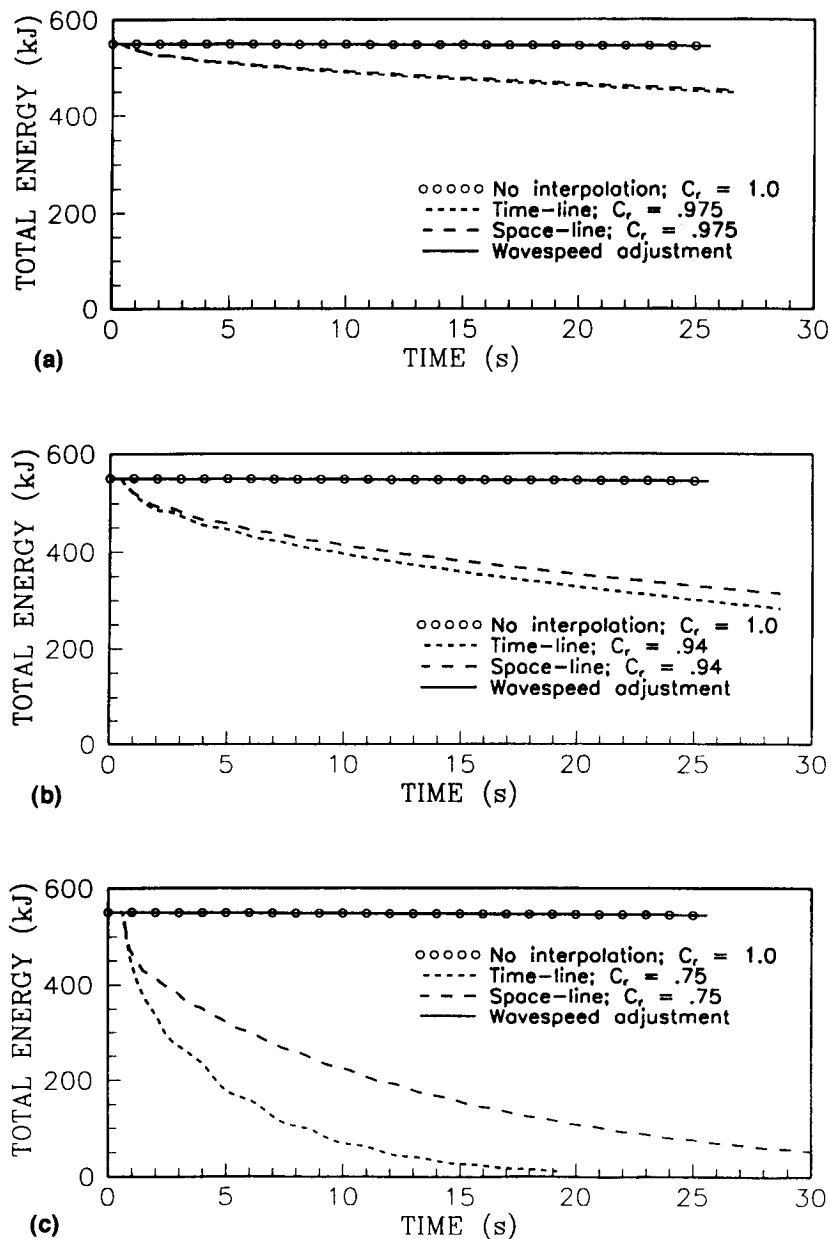


FIG. 2. Energy versus Time Plots for Case 1: Sudden Complete Valve Closure

167 time steps) can be obtained from (25) as follows: $E(25)/E(0) = (0.9959)^{167} = 0.506$, which is in excellent agreement with the value obtained by simulation. In fact, the numerical results are essentially identical to those obtained from (25) for all C_r .

At the beginning of the simulation, the steady state was duplicated in order to initiate analysis—a minor complication of time-line interpolation. This duplication effectively avoids interpolation error and conserves energy for the first time step. As the simulation continues, however, the dissipation quickly becomes large but then gradually reduces as the wave profile is smoothed by the interpolation, a phenomenon not detected by Fourier analysis. Smoothing of the sharp waves by both time-line and space-line interpolation indicates that these models will cope poorly with high-frequency waves.

Numerical experiments indicate that space-line interpolation usually produces an energy diagram similar to that of time-line interpolation, but with less energy decay for all $C_r \geq 0.6$. In fact, for all C_r , the energy diagrams for space-line and time-line interpolation are virtually identical when $t \leq 1.1$ s, the time it takes for the wave to first reach the upstream reservoir.

This is to be expected since the variation of head and flow spatially and temporarily are similar for the first L/c . Once the wave interacts with the reservoir, however, the temporal variation of head and flow is more complex. Because Fourier analysis neglects dissipation at boundary conditions, its results may also be misleading.

These observations can be summarized by considering the shape parameter β^n . When $C_r = 0.975, 0.94,$ and 0.75 , the average β^n values are $0.99, 0.95,$ and 0.88 , respectively. (In fact, a β^n of 0.88 seems conservative for real systems.) For $C_r = 0.75$, both space-line and time-line interpolation rapidly drain the system energy and significantly dampen peak pressures. This suggests that interpolation must be avoided in cases of sharp transients coupled with a Courant number considerably smaller than 1.

Case 2: Sudden Partial Valve Closure

In this second example, work is performed at the downstream boundary. This is achieved by instantaneously closing the valve from a fully open position ($\tau = 1$) to a half-closed

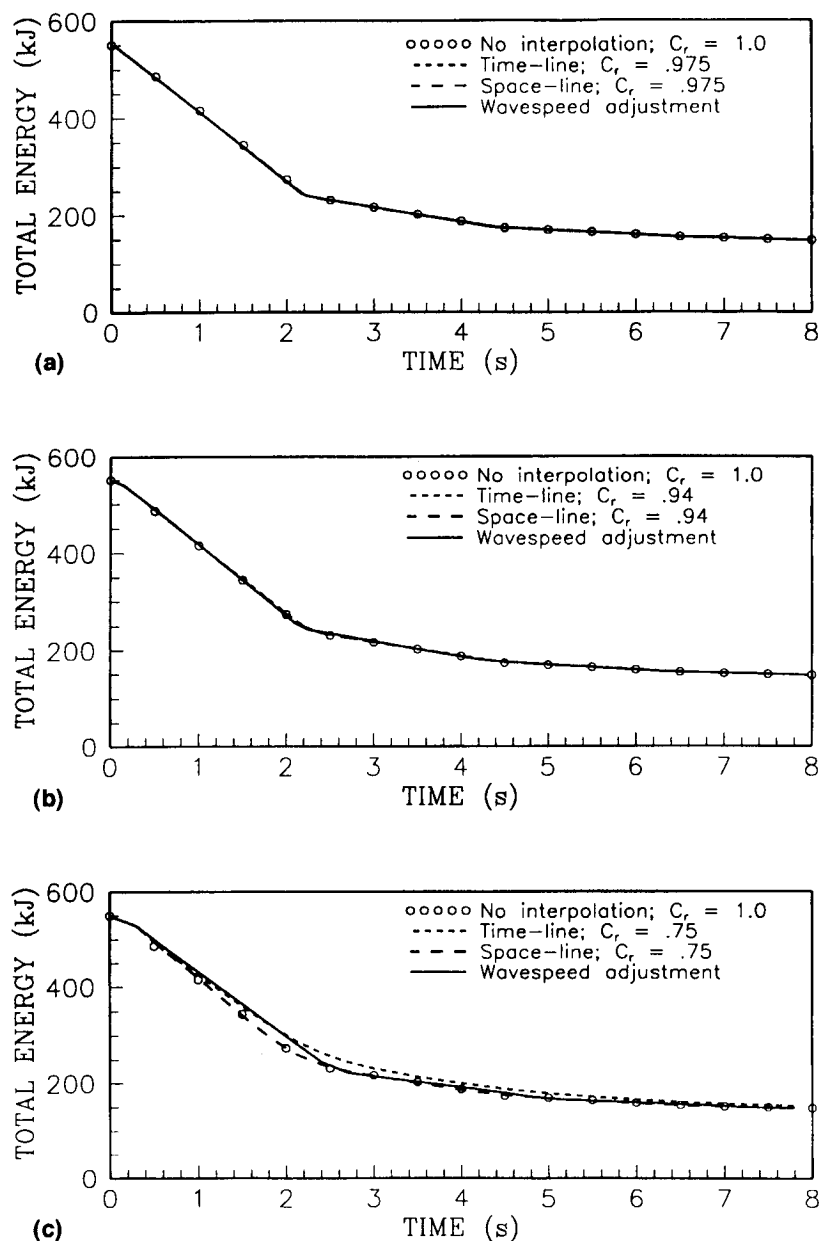


FIG. 3. Energy versus Time Plots for Case 2: Sudden Partial Valve Closure

position ($\tau = 0.5$). Fig. 3 shows that space-line interpolation produces virtually zero numerical energy dissipation as the exact and the space line energy diagram are in agreement for all simulation times and Courant numbers tested. Eqs. (14) and (16) help to explain this observation. Immediately after the sudden partial closure of the valve, a sharp wave is generated and the flow and head at the wave front are numerically dissipated, as are the kinetic and internal energy. At the same time, there is work being done by the system, as described in (16). The same numerical damping that produces less internal and kinetic energy also damps the work done by the system, giving rise to an artificial work that is too small. Numerical damping of the energy storage and of the work done by the system counterbalance each other, producing no energy dissipation. In time, the work dissipates, which smoothes the wavefront, and β^n tends to 1. As a result, the right-hand side of (18) also tends to 1, implying little additional numerical dissipation by the space-line interpolation technique.

Although Fig. 3 shows that time-line interpolation is in good agreement with the exact solution, it is still marginally less

accurate than space-line interpolation. In this case with non-zero work at the downstream end, a constant head reservoir at the upstream end, and $C_r = 0.75$, time-line interpolation tends to amplify the total energy in the system, as shown in Fig. 3(c). To understand this seemingly paradoxical increase of total energy by the time-line interpolation method, it is essential to consider what happens at the upstream boundary. The excessive smoothing of the wavefront by the time-line scheme means that the reflected negative wave from the upstream reservoir is attenuated; thus, the interpolated head does not completely arrest the flow from the reservoir into the upstream pipe, implying that there is some artificial work done by the reservoir on the pipe system and that this work is larger than the numerical dissipation. In fact, this increase in internal energy by the numerical attenuation of the wave front is similar to line packing produced in long pipelines that have high friction. This phenomena again goes undetected in the Fourier method.

Fig. 3 also shows that the wave-speed adjustment approach overpredicts the total energy of the system when the adjusted wave speed value is less than the physical wave speed. Since

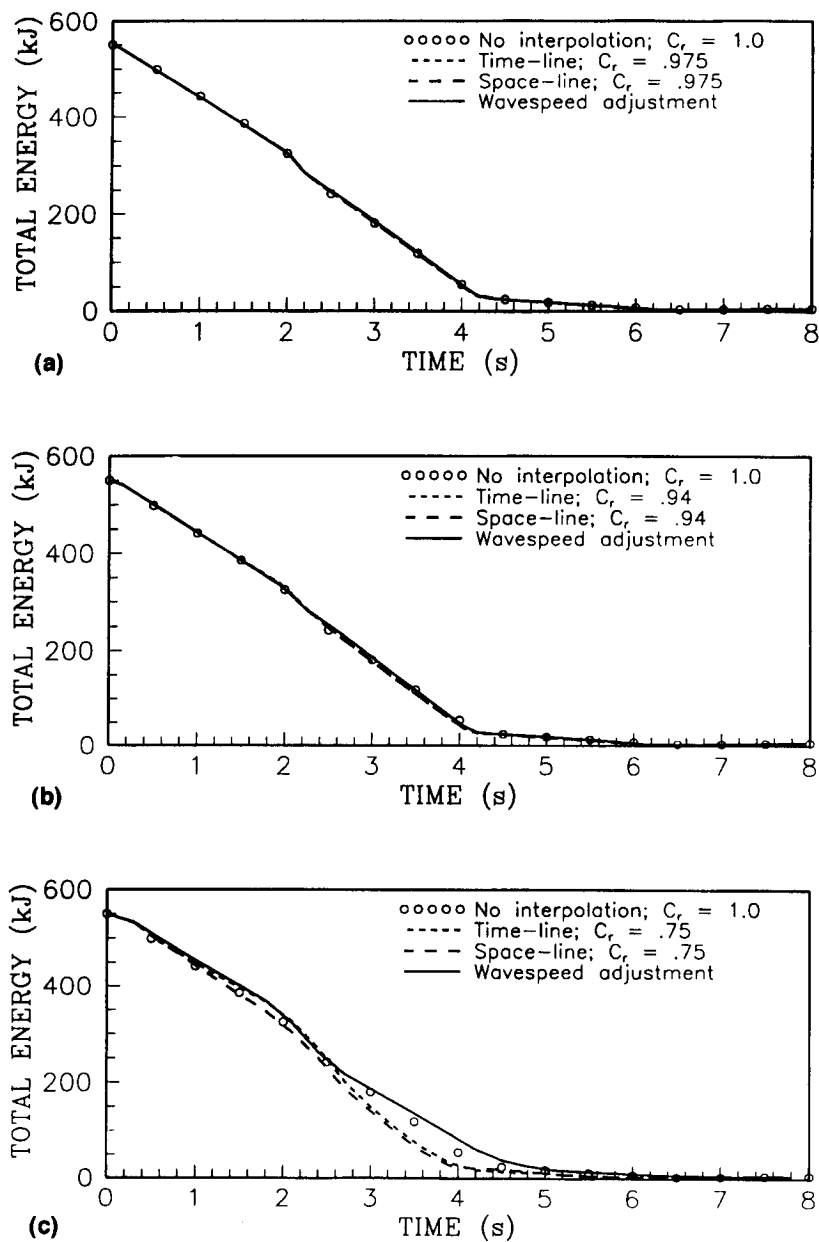


FIG. 4. Energy versus Time Plots for Case 3: Complex Valve Motion with Friction

the head change at the valve is proportional to the wave speed and the adjusted wave speed is less than the real celerity, the head change for the wave-speed adjustment method is smaller than the exact head change. As a result, the work done at the valve is less than the exact work; therefore, the total energy stored by the wave-speed adjustment method is greater than the measurement would be obtained using the physical wave speed. Therefore, the wave-speed adjustment energy diagram and the exact energy diagram differ as a result of the net work at the boundaries.

Case 3: Complex Valve Motion with Friction

In this final example, frictional energy dissipation is included by setting $f = 0.02$. In addition, physical work is performed at the boundary through a relatively more complex valve motion. More precisely, the transient is initiated by closing a valve instantaneously to a τ value of 0.55, holding this τ value constant for 2 s, and then instantaneously changing the τ value from 0.55 to 0.1 at 2 s. Thereafter, the valve opening is kept constant at $\tau = 0.1$. Figs. 4(a) and 4(b) show good agreement between all the schemes and the exact solution.

However, Fig. 4(c) shows that although the time-line and space-line results are consistent, they produce less total energy than the "exact" solution for t between 2 and 5 s. This numerical dissipation is again due to the excessive smoothing of the second sharp wave that was generated at $t = 2$ s from the second stage of the valve closure (i.e., $\tau = 0.55$ to $\tau = 0.1$). The wave-speed adjustment method overpredicts total energy for the time interval from 2 to 5 s. Again, due to the lowering of the wave speed, the work produced by this scheme is less than the actual work. Since this work comes at the expense of the total energy stored, less work implies more energy available in the system.

For $2 \text{ s} < t \leq 5 \text{ s}$, all methods converge toward the exact solution as the transient dissipates (mainly due to the work done at the boundary) and a new steady state is reached. It is interesting to note that, unlike work, frictional dissipation has only a minor influence on the behavior of the schemes tested here. This realization supports the practice of ignoring friction when theoretically comparing numerical schemes for true water hammer problems. However, the energy approach can easily analyze transient problems in which frictional dissipation is present.

CONCLUSIONS

The integrated energy relations in transient closed-conduit flow provide a method of quantifying the dissipation caused by interpolation. The energy equations developed in this paper for time-line and space-line interpolations clearly show how these schemes effectively remove significant energy from the system, particularly when wavefronts are sharp and C_r is considerably less than 1. The general rule for reducing discretization errors is to use small time steps and thus keep C_r as close to 1 as is practical.

The wave-speed adjustment approach in a limited sense preserves the total energy while distorting the partitioning of the energy between kinetic and internal forms. In addition, the wave-speed adjustment method has the following advantages over space-line and time-line techniques, particularly for problems with zero work: (1) it preserves the physical shape of the wave; (2) it is partly justified by the uncertainty associated with wave celerity; and (3) the proportional change in wave speed is often smaller than the associated degree of interpolation required by interpolation schemes. Despite these obvious merits, the wave-speed adjustment method alters the wave travel time, distorts the timing of wave interactions, and redistributes energy within the pipe system. Therefore, wave speed adjustments must be minimized whenever timing information is critical (e.g., if resonance conditions are anticipated). In such cases, the permitted adjustment in wave speed must be restricted to values much less than 15%.

In problems with nonzero work, space-line interpolation generally performs better than time-line interpolation or the wave-speed adjustment approach. This conclusion is supported by theory and by numerical experiments. The effect of work is often to smooth transient waves, which causes the shape factor β^n to tend to 1, which finally minimizes energy dissipation because the right-hand side of (14) also tends to 1.

APPENDIX I. ENERGY TERMS FOR SPACE-LINE INTERPOLATION

Using the expressions for the interpolated values of head and discharge [i.e., (12) and (13)] in a series-connected pipe system, the following inner product terms can be easily obtained:

$$\begin{aligned} \|H_R\|^2 &= \Delta x C_r^2 (H_0^n)^2 + (1 + 2C_r^2 - 2C_r) \sum_{i=1}^{m-1} (H_i^n)^2 \Delta x \\ &+ 2C_r(1 - C_r) \sum_{i=1}^{i=m-1} H_i^n H_{i-1}^n \Delta x \end{aligned} \quad (31)$$

$$\begin{aligned} \|Q_R\|^2 &= \Delta x C_r^2 (Q_0^n)^2 + (1 + 2C_r^2 - 2C_r) \sum_{i=1}^{m-1} (Q_i^n)^2 \Delta x \\ &+ 2C_r(1 - C_r) \sum_{i=1}^{i=m-1} Q_i^n Q_{i-1}^n \Delta x \end{aligned} \quad (32)$$

$$\begin{aligned} \|H_S\|^2 &= \Delta x C_r^2 (H_m^n)^2 + (1 + 2C_r^2 - 2C_r) \sum_{i=1}^{m-1} (H_i^n)^2 \Delta x \\ &+ 2C_r(1 - C_r) \sum_{i=1}^{i=m-1} H_i^n H_{i+1}^n \Delta x \end{aligned} \quad (33)$$

$$\begin{aligned} \|Q_S\|^2 &= \Delta x C_r^2 (Q_m^n)^2 + (1 + 2C_r^2 - 2C_r) \sum_{i=1}^{m-1} (Q_i^n)^2 \Delta x \\ &+ 2C_r(1 - C_r) \sum_{i=1}^{i=m-1} Q_i^n Q_{i+1}^n \Delta x \end{aligned} \quad (34)$$

The inner produce terms required to expand (9) are

$$\begin{aligned} \langle H_R, Q_R \rangle - \langle H_S, Q_S \rangle &= \frac{\Delta x}{2} [H_{R_1} Q_{R_1} - H_{S_{m-1}} Q_{S_{m-1}} \\ &+ (2C_r - 1)(H_1 Q_1 - H_{m-1}^n Q_{m-1}^n)] \end{aligned} \quad (35)$$

The boundary terms are given by

$$\begin{aligned} (Q_m^{n+1})^2 + \left(\frac{1}{B}\right)^2 (H_m^{n+1})^2 &= -\frac{2}{B} Q_m^{n+1} H_m^{n+1} + \frac{2}{B} Q_{R_m}^n H_{R_m}^n \\ &+ Q_{R_m}^2 + \left(\frac{1}{B}\right)^2 H_{R_m}^2 \end{aligned} \quad (36)$$

$$\begin{aligned} (Q_0^{n+1})^2 + \left(\frac{1}{B}\right)^2 (H_0^{n+1})^2 &= \frac{2}{B} Q_0^{n+1} H_0^{n+1} - \frac{2}{B} Q_{S_1}^n H_{S_1}^n \\ &+ Q_{S_1}^2 + \left(\frac{1}{B}\right)^2 H_{S_1}^2 \end{aligned} \quad (37)$$

Substituting these into (9) and using the common heads and discharges at pipe junctions to simplify yields (14).

APPENDIX II. REFERENCES

- Chaudhry, M. H. (1987). *Applied hydraulic transients*. Van Nostrand Reinhold, New York, N.Y.
- Chaudhry, M. H., and Hussaini, M. Y. (1985). "Second-order accurate explicit finite-difference schemes for waterhammer analysis." *J. Fluid Engng.*, 107(4), 523-529.
- Damuller, D. C., Bhallamudi, S. M., and Chaudhry, M. H. (1989). "Modeling unsteady flow in curved channel." *J. Hydr. Engng.*, ASCE, 115(11), 1471-1495.
- Ghidaoui, M. S., and Karney, B. W. (1994). "Equivalent differential equations in fixed-grid characteristics method." *J. Hydr. Engng.*, ASCE, 120(10), 1159-1175.
- Ghidaoui, M. S., and Karney, B. W. (1995). "Modified transformation and integration of 1-D wave equations." *J. Hydr. Engng.*, ASCE, 121(10), 758-760.
- Goldberg, D. E., and Wylie, E. B. (1983). "Characteristics method using time-line interpolations." *J. Hydr. Engng.*, ASCE, 109(5), 670-683.
- Karney, B. W. (1990). "Energy relations in transient closed-conduit flow." *J. Hydr. Engng.*, ASCE, 116(10), 1180-1196.
- Karney, B. W., and Ghidaoui, M. S. (1992). "Discussion of 'Spline interpolations for water hammer analysis,' by Sibetheros, I. A., Holley, E. R., and Branski, J. M." *J. Hydr. Engng.*, ASCE, 118(11), 1597-1600.
- Karney, B. W., and Ghidaoui, M. S. (1997). "Flexible discretization algorithm for fixed-grid MOC in pipeline systems." *J. Hydr. Engng.*, ASCE, 123(10), 1004-1011.
- Karney, B., and McInnis, D. (1992). "Efficient calculation of transient flow in simple pipe networks." *J. Hydr. Engng.*, ASCE, 118(7), 1014-1030.
- O'Brian, G. G., Hyman, M. A., and Kaplan, S. (1951). "A study of the numerical solution of partial differential equations." *J. Math. Phys.*, 29(4), 223-251.
- Samuels, G. P., and Skeels, P. C. (1990). "Stability limits for Preissmann's scheme." *J. Hydr. Engng.*, ASCE, 116(8), 997-1011.
- Sibetheros, I. A., Holley, E. R., and Branski, J. M. (1991). "Spline interpolations for water hammer analysis." *J. Hydr. Engng.*, ASCE, 117(10), 1332-1349.
- Wiggert, D. C., and Sundquist, M. J. (1977). "Fixed-grid characteristics for pipeline transients." *J. Hydr. Engng.*, ASCE, 103(12), 1403-1415.
- Wylie, E. B., and Streeter, V. L. (1993). *Fluid transients in systems*. Prentice Hall, Englewood Cliffs, N.J.

APPENDIX III. NOTATION

The following symbols are used in this paper:

- A = cross-sectional area of pipe;
- B = pipe constant c/gA ;
- c = wave speed or celerity;
- \bar{c} = adjusted wave speed or celerity;
- C_r = Courant number;
- d = derivative;
- D = energy dissipation;
- D' = rate of energy dissipation;

D_o = pipe diameter;
 E = sum of total kinetic energy and total internal energy;
 E^n = sum of total kinetic energy and total internal energy at time level n ;
 f = Darcy-Weisbach friction factor;
 f^\pm = friction factor along C^+ and C^- characteristics;
 g = acceleration due to gravity;
 H = piezometric head, $H = H(x, t)$;
 H_i^n = piezometric head at node i and time level n ;
 H_R, H_S = piezometric head at interpolation points R and S , respectively;
 i = spatial nodal location;
 L = pipe length along centerline;
 m = number of reaches in a particular pipe;
 n = time nodal location;
 N_p = number of reaches in a pipe p ;
 N_{Sp} = number of reaches in pipe with minimum L/c ;
 p = pipe index;
 Q = volumetric flow function, $Q = Q(x, t)$;
 Q_i^n = volumetric flow at node (n, i) ;
 Q_R, Q_S = piezometric head at interpolation points R and S , respectively;

t = time;
 x = space coordinate along centerline;
 T, \bar{T} = total kinetic energy with wave speed c and \bar{c} , respectively;
 U, \bar{U} = total potential energy with wave speed c and \bar{c} , respectively;
 W', \bar{W}' = rate work is done when wave speed is c and \bar{c} , respectively;
 β = profile function for space-line interpolation;
 γ = profile function for energy expression;
 Δ = change in a quantity;
 Δt = time step;
 Δx = space increment;
 ζ = arbitrary function defined on spatial domain;
 ξ = time-line interpolation distance;
 ρ = fluid density;
 τ = dummy variable for time integration;
 ϕ = index of compressibility;
 ψ = arbitrary function defined on spatial domain;
 \pm = positive and negative characteristics;
 $| \cdot |$ = absolute value function;
 $\| \cdot \|$ = norm function; and
 $\langle \cdot \rangle$ = inner product function.